

Computation of Optical Energy Band Gaps of Double Alkali Tetraborate Glasses Containing Alkaline Earth Oxide

Sarap Krishnaprasad¹, Md. Shareefuddin¹, and Gokarakonda Ramadevudu^{2*}

¹Department of Physics, Osmania University, Telangana, Hyderabad, India-500007

²Department of Physics, Vasavi College of Engineering (A), Telangana, Hyderabad, India-31

*Corresponding author e-mail: dr.ramdev@gmail.com

ABSTRACT

The main object of the present work is to compute optical energy band gap values using various methods, find plasma frequency, evaluate excitation energy for electronic transitions (E_d) and dispersive energy (E_o) of alkaline earth oxide containing double tetraborate glasses. The glass samples $10\text{MgO}-30\text{ZnO}-x\text{Li}_2\text{B}_4\text{O}_7-(60-x)\text{K}_2\text{B}_4\text{O}_7$ (MZLK) and $10\text{CaO}-30\text{ZnO}-x\text{Li}_2\text{B}_4\text{O}_7-(60-x)\text{K}_2\text{B}_4\text{O}_7$ (SZLK) ('x' changes from 0 to 60 mol%) are synthesized using melt quenching procedure. These glass systems are characterized by optical absorption spectroscopy. The optical constants of these glasses are determined over a spectral range. The optical band gap energies evaluated by ASF method varied from 3.19 to 3.45 for MZLK glasses and 3.36 to 3.43 for CZLK glass samples. The ratio of average carrier concentration to effective mass for CZLK glasses increased with increasing mole% of $\text{Li}_2\text{B}_4\text{O}_7$ in the glass matrix. The enhancement in reflectance (R) is attributed to an increase in refractive index value. ZnO containing glasses show good optical properties. Alkaline earth oxide modifies the glass network. Hence alkali tetraborate glasses undergo significant structural changes and give better physical, optical, and electrical properties. The optical band gap energies can be tailored by varying any one of the alkali tetraborates in the glass composition.

Key Words: alkali tetra borates, optical bandgap energy, dielectric constant, plasma frequency, excitation energy, dispersive energy.

Introduction: The history of glass dates back about five thousand years [1]. It has become one of the most important inventions in the lives of human beings. Glasses are not only useful for eye-sight correction, but the modern glasses play very intriguing role in various fields including windscreens, bottling, illumination, solid electrolytes, solar cells, bioactive glasses, radiation guarding, optical fibers, laser media, display devices, non-linear optics, sensors, smart glasses and several more [2-6].

It is established that structural changes play a key role in controlling parameters like band gap, Urbach energies, density, molar volume, refractive index, dielectric constant etc. The optical absorption edge also undergoes either a red shift or a blue shift. Such involved changes help to manufacture many optical devices utilizing these glass materials. The optically induced transitions due to optical absorption are important in understanding band structure and optical energy gap of glasses [7].

Borate glasses especially alkali and alkaline borate glasses show very interesting glass structure due existence of several structural units like boroxol groups, penta-borates, di-borates consisting triangular $[\text{BO}_3]$ and tetrahedral $[\text{BO}_4]$ coordinated groups along with ring-type and chain-type metaborate groups [8]. The present tetraborate glasses are also expected to consist of the above-

mentioned similar structural groupings which significantly alter the optical characteristics. The alkaline earth oxide (like MgO and CaO) at low mole percent breaks the glass network and modifies it. ZnO is good metal oxide that brings in excellent optical properties and enhances the stability of the borate glasses.

Oxide glasses, especially silicate, borosilicate, and other glasses containing heavy metal oxides containing Al_2O_3 etc., have immense industrial and technical applications [9]. Special glasses for various industrial applications like sealing glasses, good corrosion resistance, excellent hermeticity, minimal thermal expansion etc., have been developed such as CABAL (Calcium-boro-aluminate) glass, Mixed alkali-barium-alumino-phosphate glass etc., [10-12].

The present work aims to compute optical band gap energies of alkaline earth oxide containing double tetraborate glasses. This paper discusses the impact of varying content of one of the tetraborate oxides on the optical properties. The study reports plasma frequency, ratio of average carrier concentration to effective mass and other parameters.

Materials and Methods:

In the present study, $10\text{MgO}-30\text{ZnO}-x\text{Li}_2\text{B}_4\text{O}_7-(60-x)\text{K}_2\text{B}_4\text{O}_7$ (MZLK) and $10\text{CaO}-30\text{ZnO}-x\text{Li}_2\text{B}_4\text{O}_7-(60-x)\text{K}_2\text{B}_4\text{O}_7$ (CZLK) ('x' changes from 0 to 60 mol%) were prepared by melt quenching. The alkaline earth oxide (MgO or CaO) and ZnO were fixed respectively at 10 mole% and 30 mol% in the glass composition, where as one of the alkali tetraborates gradually changed from 0 mole% to 60 mol%. Glasses were prepared from high quality chemicals zinc oxide (ZnO), magnesium oxide (MgO), Calcium oxide (CaO), lithium tetraborate ($\text{Li}_2\text{B}_4\text{O}_7$) and potassium tetraborate ($\text{K}_2\text{B}_4\text{O}_7$) (Sigma-Aldrich). A batch of 10g of the above starting materials were weighed, grounded, and melted in a porcelain crucible at about 1100°C temperature in a micro-controlled electrical furnace for more than 30 minutes. The melt was spun often so that a uniform mixture was obtained. The homogenous and uniformly melted mixture was quickly transferred onto a heated (around 200°C) stainless steel plate and made the melt into a different shape by pressing it with a preheated steel rod. The glass samples were transparent, clear without any air bubbles. All the glass samples were annealed at 200°C for a duration of about 12 hours so that any stress remained are relieved. The optical absorption spectra for all the polished glass samples of about 1mm thick were scanned on Agilent Technologies-Carry 5000 with UMA Spectrophotometer in the wavelength region 200 to 1100 nm. The band position accuracy in its measurement is about $\pm 1\text{nm}$. Table.1 shows the glass samples composition in mole percentage. Figure.1 depicts X-ray diffraction patterns of some MZLK and CZLK glass samples.

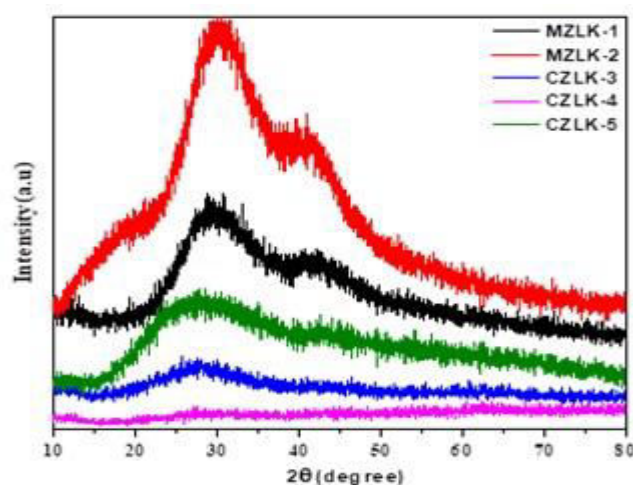


Fig.1 X-ray diffraction patterns of some MZLK and CZLK glass samples

RESULTS AND DISCUSSION:

At lower wavelengths glasses show higher optical absorption compared to higher wavelengths. There is an ultraviolet cut-off wavelength at which the absorption coefficient increases instantaneously known as fundamental absorption edge. Generally below 200nm, oxide glasses instead of transparent, behave as opaque since the incident photo energy is more than the optical band gap energy. Hence the energy band gap between the conduction and valence bands can be measured using optical absorption spectra of oxide glasses. Like in crystalline semiconductors the band transitions may direct or indirect allowed transitions are also possible in glasses.

Table.1 Composition of 10MO-30ZnO-xLi₂B₄O₇-(60-x)K₂B₄O₇ (M=Mg, Ca) glasses

Glass code	MgO	CaO	ZnO	Li ₂ B ₄ O ₇	K ₂ B ₄ O ₇
MZLK-1	10	-	30	0	60
MZLK-2	10	-	30	15	45
MZLK-3	10	-	30	30	30
MZLK-4	10	-	30	45	15
MZLK-5	10	-	30	60	0
CZLK-1	-	10	30	0	60
CZLK-2	-	10	30	15	45
CZLK-3	-	10	30	30	30
CZLK-4	-	10	30	45	15
CZLK-5	-	10	30	60	0

The optically induced transitions help to know band structure and optical energy gap of glasses can be computed. The optical absorption coefficient (α) is usually estimated with the help of optical absorbance. The optical absorption spectra of some of the samples are shown in figure.2. All other samples have shown similar optical absorption spectra. The absorption coefficient (α) in terms of thickness of the glass and Transmittance(T), Reflectance(R) can be expressed as

$$\alpha = \left(\frac{1}{t}\right) \ln\left(\frac{1-R}{T}\right) \quad (1)$$

Fig.3 represents transmittance and reflectance spectra of MZLK and CZLK glass samples in the wavelengths between 200nm and 1100 nm. The cutoff wavelength of MZLK and CZLK glasses are calculated and are presented in Table.2 and 3 respectively. It is observed that the UV absorption edge is violet shifted with increasing x mol% of Li₂B₄O₇ content from approximately 407 nm to 383 nm.

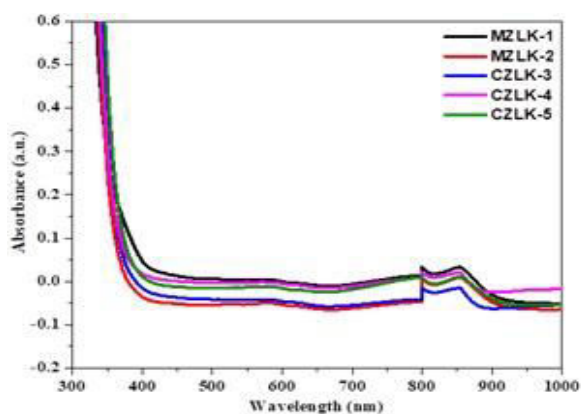


Fig. 2: Optical absorption spectra of some MZLK and CZLK Glasses.

Absorption coefficient (α) is correlated to photon energy and optical band gap energy E_{opt} as proposed by Mott and Tauc in the following expression for amorphous materials [13-14].

$$[h\nu\alpha(\nu)]^m = B(h\nu - E_{opt}) \tag{2}$$

here optical band gap is E_{opt} , α is absorption coefficient, h is Planck's constant, (ν) is frequency of incident photons, B is a constant and 'm' is an index associated with various optical transitions. The kind of transitions are either direct or indirect transitions. The assigned transitions are given as indirect allowed ($m=1/2$), indirect forbidden ($m=1/3$), direct allowed ($m=2$), direct forbidden ($m=3$). In a crystalline semiconductor both energy and momentum of an electron must be conserved during optical transitions. In amorphous materials like glasses energy is only conserved. Many oxide glasses exhibiting indirect allowed transitions near the band edge E_g , emissions or absorption of photon are assisted phonons (phonon assisted transitions).

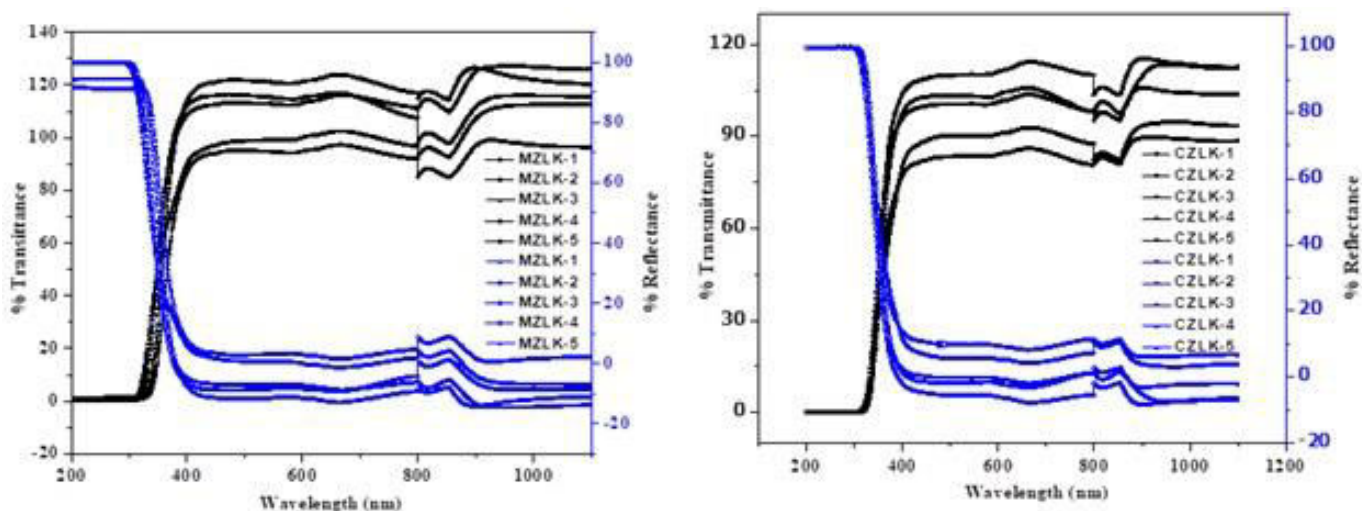


Fig.3: The transmittance and Reflectance spectra of MZLK and CZLK Glass systems

The optical energy band gap (E_{opt}) can be computed from the plot $(\alpha h\nu)^m$ vs photon energy ($h\nu$) for the transitions mentioned above. E_{opt} values are attained by drawing tangents to the linear portion of these plots and extrapolating them on to x-axis as shown in Fig.4&5. The optical band gap energy thus evaluated for the glass samples at different values of m is listed in Table.1. The optical band gap values vary depending on exponent m values and hence best fit plot that satisfies 'm' value shall be considered for taking band gap values. Therefore, the Eq. (2) helps to resolve the type of transitions.

Absorption Spectrum Fitting (ASF) method is also used to evaluate optical energy band gap $E_{opt}(ASF)$. The values $E_{opt}(ASF)$ are determined from the graph (Fig.5) between $(\alpha/\lambda)^{1/2}$ vs $(1/\lambda)$. The cut-off wavelength values (λ_c) is calculated by extrapolating the linear region of the plot $(\alpha/\lambda)^2$ and $(1/\lambda)^{-1}$ at $(\alpha/\lambda)^2 = \text{zero}$ for both MZLK and CZLK glass samples without the requirement of glass sample thickness (t). The $E_{opt}(ASF)$ are computed using cut-off wavelength values (λ_c) by following relation:

$$E_{opt} = \frac{hc}{\lambda_c} = \frac{1239.83}{\lambda_c} \tag{3}$$

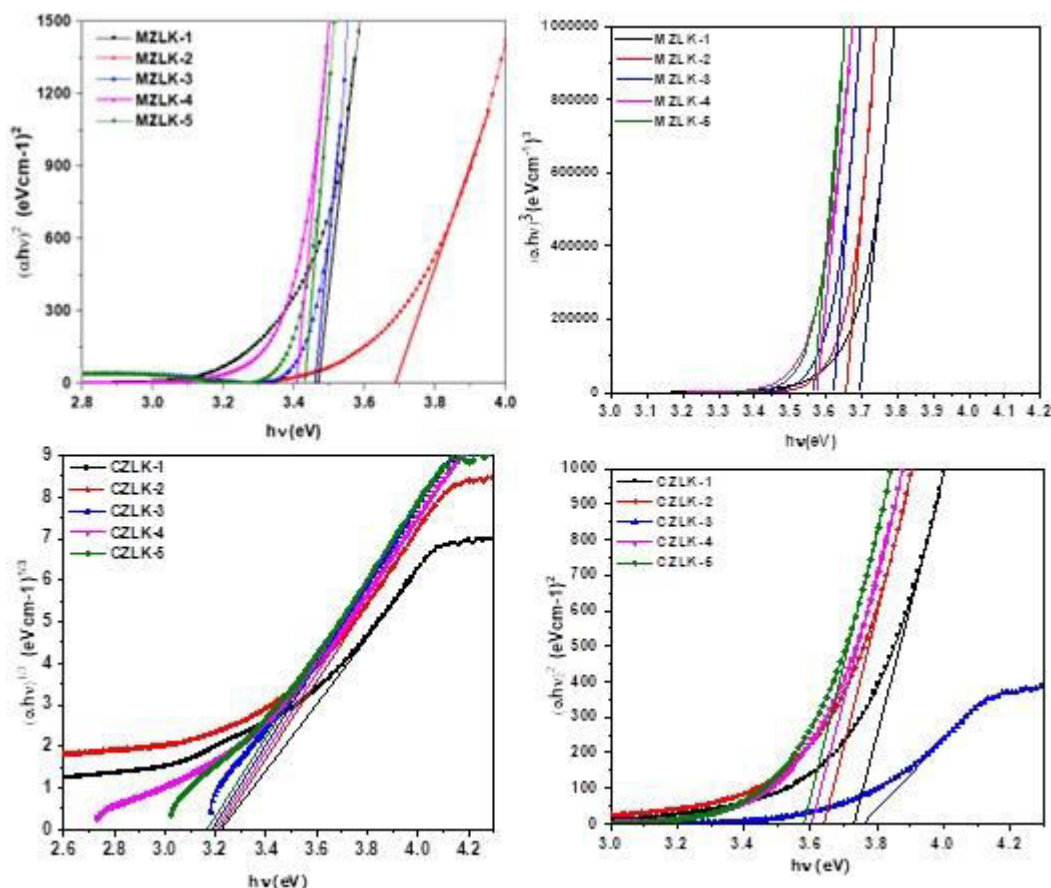


Fig.4. Plots between $(\alpha hv)^m$ and photon energy hv for $m=1/3,2$ and 3 of MZLK and CZLK glasses.

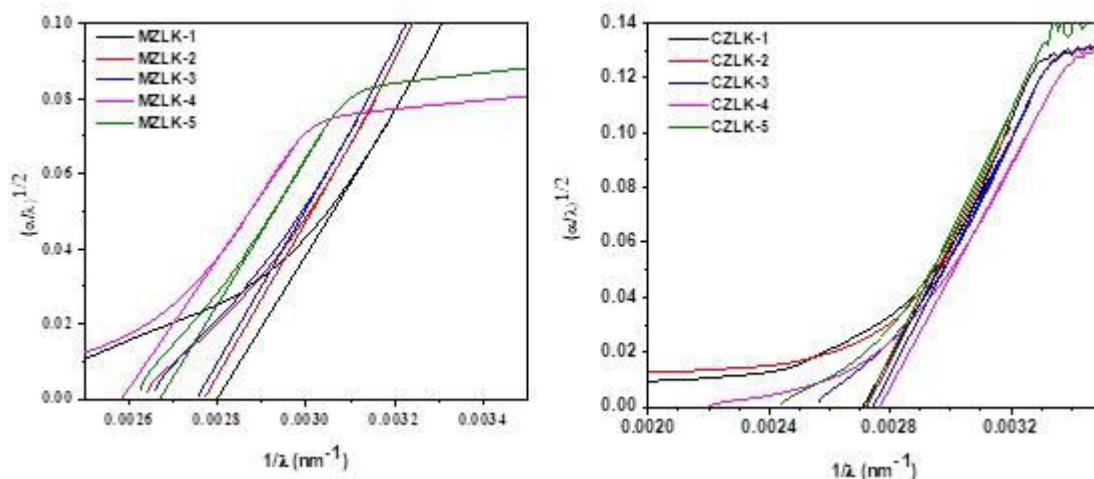


Fig.5. A graph between $(\alpha/\lambda)^{1/2}$ and $(1/\lambda)$ to estimate $E_{opt}(ASF)$

The optical energy band gap of a glass can also be computed through determining imaginary part of dielectric constant (ϵ_2) with appropriate exponent value (m). The optical properties shown by a glass are the function of its complex refractive index and dielectric constant. The extinction coefficient describes the attenuation of the intensity of incident light i.e. electromagnetic wave amplitude while propagating in a medium. The optical properties of glass, in general for any solid material, is dependent on light-matter interaction.

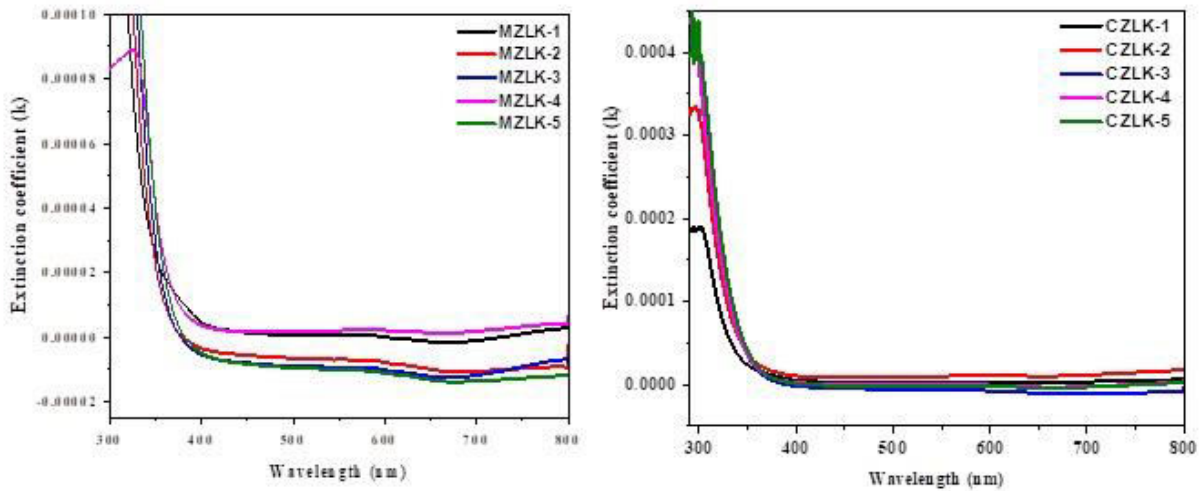


Fig.6. Plots between extinction coefficient and wavelength

Hence decay of electromagnetic energy of the interacted light is specified by the extinction coefficient of a material which represents how fast the light is absorbed by a material. In glassy materials extinction coefficient is a function of structural units present in it. Refractive index 'n' and extinction coefficient 'k' are theoretical related to reflection coefficient or reflectivity (R). According to this theory, the reflectance of light from a material can be written as [15]

$$\text{Extinction coefficient } k = \frac{\alpha \lambda}{4\pi} \tag{4}$$

$$n^2 = \frac{1+R^{1/2}}{1-R^{1/2}} \tag{5}$$

here R is reflectivity in the transparent region of the glass sample. Fig.6 illustrates the plots between extinction coefficient as a function of wavelength. The optical band gap energies computed from ASF method and from the imaginary part of dielectric constant (ϵ_2) are listed in Table.2. There exists a relationship between real (ϵ_1) and imaginary (ϵ_2) parts of dielectric constant as stated below:

$$\epsilon_1 = n^2 - k^2 \tag{6}$$

$$\epsilon_2 = 2nk \tag{7}$$

Table.2. Cut off wavelength (λ_c) and optical energy gap (E_{opt})

Glass Code	λ_c (nm)	E_{opt} (eV) for 'm ='				$E_{opt}(ASF)$ (eV)	$E_{opt}(\epsilon_2)$ (eV)
		1/2	1/3	2	3		
MZLK-1	405	3.40	3.29	3.46	3.69	3.45	3.75
MZLK-2	370	3.37	3.26	3.68	3.65	3.43	3.70
MZLK-3	374	3.35	3.22	3.45	3.62	3.40	3.66
MZLK-4	382	3.22	3.04	3.40	3.57	3.19	3.51
MZLK-5	384	3.29	3.12	3.43	3.56	3.31	3.60
CZLK-1	407	3.67	3.22	3.72	3.89	3.37	3.66
CZLK-2	387	3.57	3.21	3.64	3.79	3.38	3.59
CZLK-3	375	3.53	3.18	3.76	3.76	3.40	3.60
CZLK-4	370	3.55	3.20	3.60	3.77	3.43	3.58
CZLK-5	383	3.52	3.17	3.58	3.74	3.36	3.56

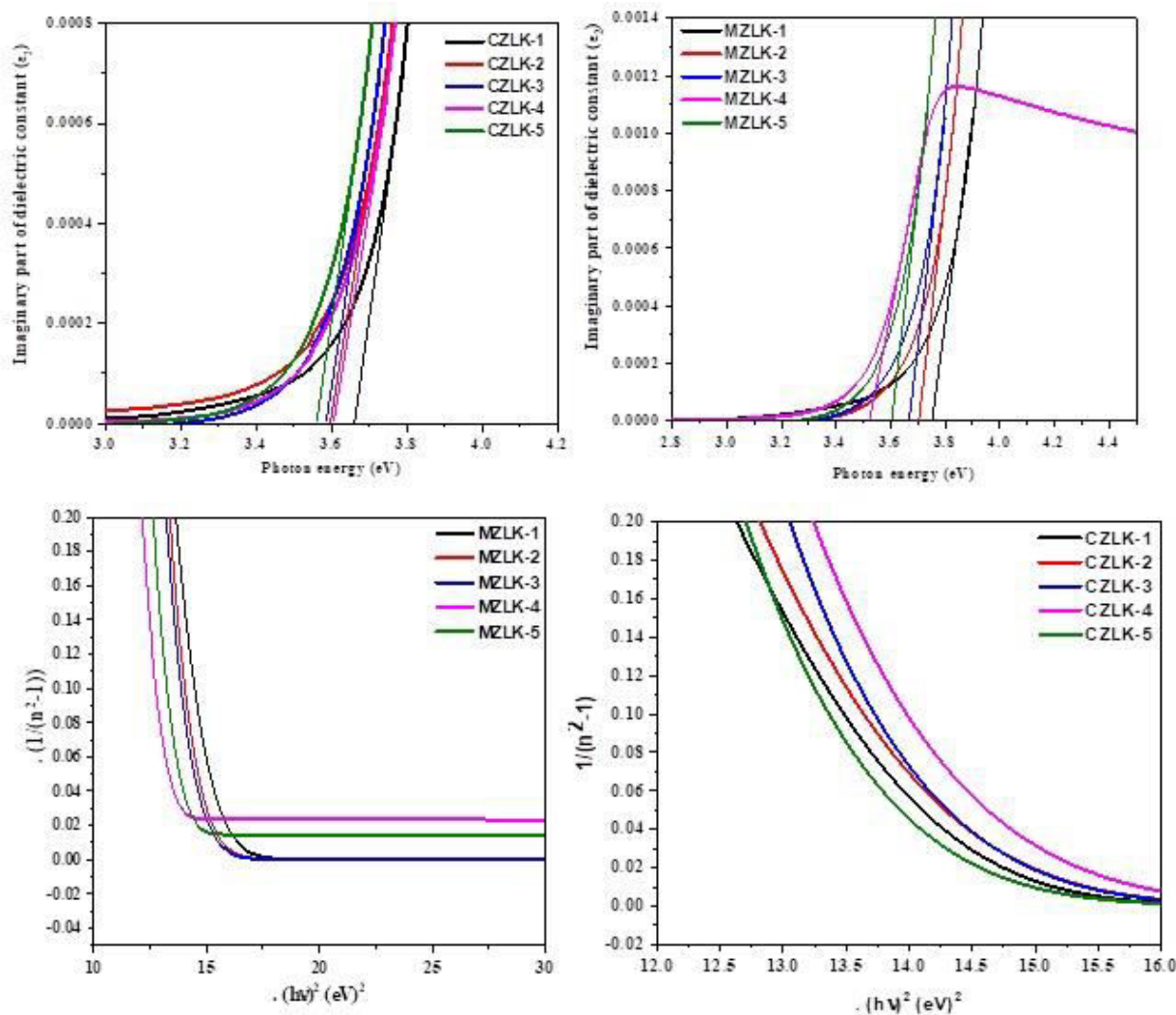


Fig.7. Variation of imaginary part of the dielectric constant with and photon energy and $1/(n^2-1)$ with $(h\nu)^2$

Fig.7 shows variation of the real part of dielectric constants with the photon energy and $1/(n^2-1)$ with $(h\nu)^2$. A steady exponential increment in both real and imaginary dielectric constants values with increasing energy of incident photons is observed. The optical energy band gap, $E_g(\epsilon_2)$ is obtained by extrapolation of imaginary part of the dielectric constant (ϵ_2) to zero as shown in the fig.7.

The real part of dielectric constant can be expressed according to theory of dielectrics proposed by Drude as:

$$\epsilon_1 = n^2 - k^2 = \epsilon_\infty - \left(\frac{e^2}{4\pi^2 c^2 \epsilon_0}\right) \left(\frac{N_c}{m^*}\right) \lambda^2 \tag{8}$$

The plasma resonance frequency from the above expression can be written as:

$$\omega_p^2 = \left(\frac{e^2}{\epsilon_0 \epsilon_\infty}\right) \left(\frac{N_c}{m^*}\right) \tag{9}$$

Table.3. Ratio of free carrier concentration to effective mass (N/m^*), high frequency dielectric constant (ϵ_∞), plasma resonance angular frequency (ω_p), plasma wavelength (λ_ω), average excitation energy for electronic transitions (E_o), dispersive energy (E_d) values.

Glass Code	$N/m^* \cdot 10^{59}$ ($Kg^{-1} m^{-3}$)	ϵ_∞	ω_p $\times 10^{15}$ (Hz)	$\lambda_\omega \times 10^2$ (nm)	E_d (eV)	E_o (eV)
MZLK-1	7.42	74.23	5.37	3.50	2.71	3.95
MZLK-2	7.38	75.45	5.31	3.54	2.42	3.88
MZLK-3	7.72	79.43	5.30	3.55	2.33	3.85
MZLK-4	7.27	81.23	5.08	3.70	2.07	3.68
MZLK-5	8.63	91.72	5.21	3.61	2.29	3.76
CZLK-1	6.57	71.03	5.17	3.64	2.26	3.78
CZLK-2	7.42	78.36	5.23	3.59	2.17	3.79
CZLK-3	8.92	91.64	5.30	3.55	1.71	3.78
CZLK-4	8.61	87.4	5.33	3.52	1.95	3.83
CZLK-5	9.54	99.85	5.25	3.58	1.82	3.74

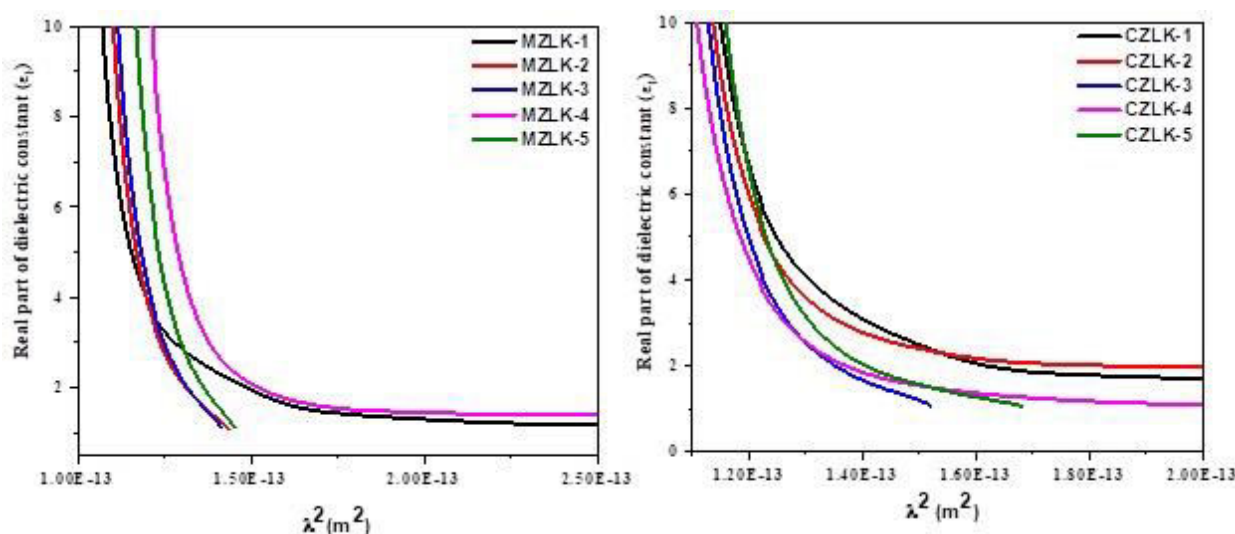


Fig.8 Variation of real part of the dielectric constant (ϵ_1) with λ^2

Here, ϵ_∞ -high frequency dielectric constant and (N_c/m^*) - ratio of carrier concentration to carrier effective mass. Fig. 8 represents variation of ϵ_1 with λ^2 . The values of (N_c/m^*) and ϵ_∞ are evaluated respectively from the slope and intercept of ϵ_1 with λ^2 graph. The plasma resonance frequency ω_p , is estimated from these calculated values and reported in Table.3. The change in refractive index with photon energy can be described by single oscillator approximation as given by [7]

$$n^2 - 1 = \frac{E_d E_o}{[E_o^2 - E^2]} \tag{10}$$

Here dispersion energy (E_d) and average excitation energy (E_o) of electronic transitions have usual meanings and the photon energy, $E=hv$. The values of E_o and dispersive energy (E_d) are evaluated from the linear fit of $1/(n^2-1)$ versus $(hv)^2$ plots (Fig. 7) and are listed in Table.3.

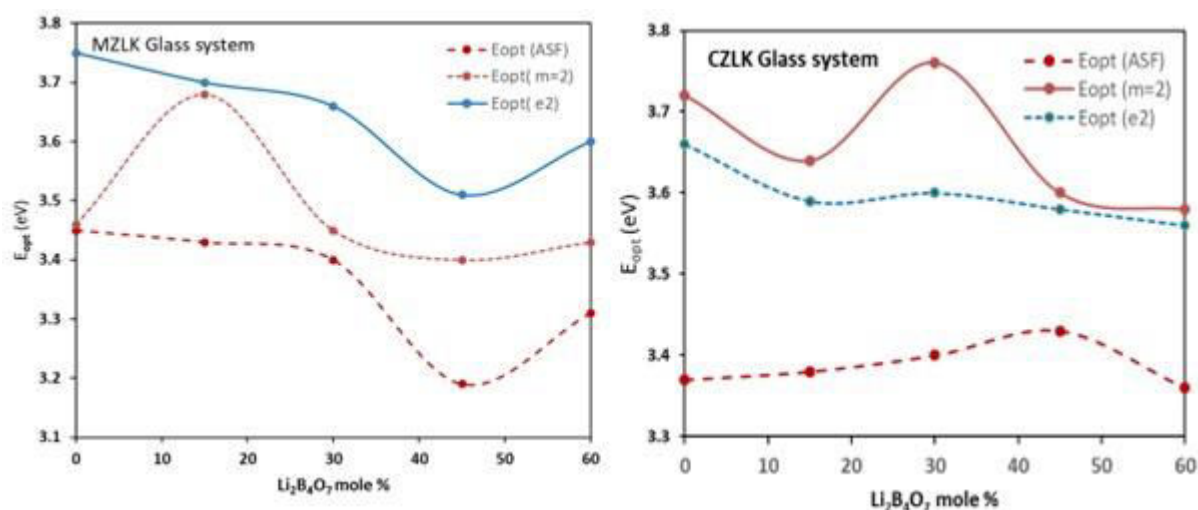


Fig.9 Variation of E_{opt} with $Li_2B_4O_7$ mole %.

The results presented above reveal that optical energy band gap values show a non-linear behaviour with increasing $Li_2B_4O_7$ content in the glass composition. The optical band gap values of the glass system MZLK are slightly greater compared to CZLK glasses. The average values of electronic energy gap E_o and dispersive energy (E_d) values are also higher for MZLK glasses. It is observed that ϵ_1 increases with $Li_2B_4O_7$ content. The optical energy band gap values estimated from absorption spectra from indirect allowed transition are in line and comparable with the values estimated from the dielectric measurements ϵ_2 . Hence indirect allowed electronic transitions are attributed as the best transition models for the present glass samples.

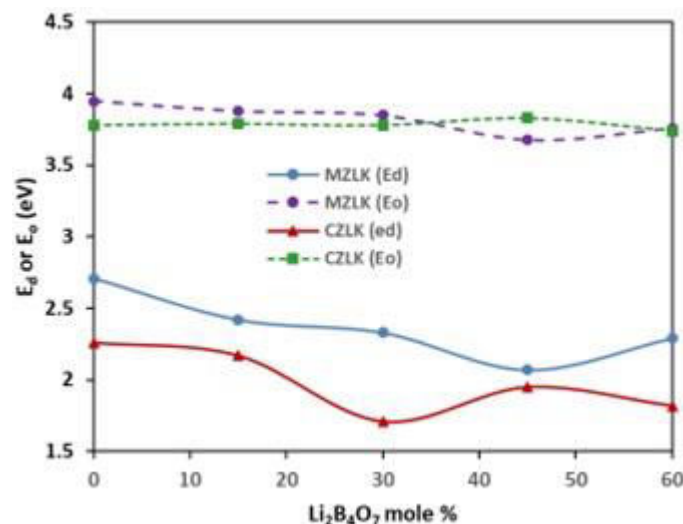


Fig.10 Variation of E_d and E_o with $\text{Li}_2\text{B}_4\text{O}_7$ mole %.

The values of $\frac{N_c}{m^*}$ reflected almost increasing trend except with small inflections with an increase in $\text{Li}_2\text{B}_4\text{O}_7$ content. Thereby the reflectance (R) also increased. Increased reflectance caused an enhancement in the refractive index values. The calculated wavelength λ_o corresponding to the plasma frequency ω_p of MZLK glasses have shown a shift towards longer wavelength whereas CZLK glass system exhibited a shift towards shorter wavelengths with increasing mole% of $\text{Li}_2\text{B}_4\text{O}_7$.

The variation of optical band gap energies and excitation energy (E_o) and dispersive energy (E_d) have shown inflection point from the linearity when the mole % of two alkali tetra borate oxides in the glass composition are equal i.e. $x=30$ mole%. Such type of behaviour is generally shown by mixed alkali borate glasses and the effect is termed as “mixed alkali effect (MAE) [16-18]. The non-linearity shown by the glass samples in the optical properties are attributed to the progressive substitution of Li atoms in place of K atoms. This substitution of atoms might cause more stress because of insertion of Li atoms. The overall stress encountered by K and (or) Li atoms might have reached optimal value at $\text{Li} = \text{K}$ [19]. The observed non-linear alteration and inflection with substitution of $\text{Li}_2\text{B}_4\text{O}_7$ caused considerable structural adjustments and is attributed to mixed alkali effect. The non-linear changes can also be attributed to ionic sizes of the alkali and alkaline ions. The sizes of Li^+ ion (0.076nm), K^+ (0.138nm), Mg^{2+} (0.072nm), Ca^{2+} (0.099nm), Zn^{2+} (0.060nm four coordinated) indicate that smaller metal ions like Mg^{2+} and Zn^{2+} might have taken interstitial or void locations. The reason for MZLK glass systems showing slightly higher optical energy band gap values is because of lower ionic size of Mg^{2+} compared to Ca^{2+} ion. Hence there is competition between ions present in the glass network to occupy various structural locations. Thus, the computed optical energy band gaps of double alkali tetraborate glasses containing alkaline earth oxides are structure dependent.

CONCLUSIONS

The glasses with general formulae $10\text{MgO}-30\text{ZnO}-x\text{Li}_2\text{B}_4\text{O}_7-(60-x)\text{K}_2\text{B}_4\text{O}_7$ and $10\text{CaO}-30\text{ZnO}-x\text{Li}_2\text{B}_4\text{O}_7-(60-x)\text{K}_2\text{B}_4\text{O}_7$ with mole% of ‘x’ changing from 0 mol% to 60 mol% were prepared by melt quench process. The following conclusions are drawn from the present studies:

- The optical energy band gap values are computed using different methods such as Tauc’s, ASF and from the imaginary part of dielectric constant (ϵ_2).

- The E_{opt} values estimated from absorption spectra with exponent 'm=1/2' corresponding to indirect allowed transition agree with the values estimated from the imaginary part of dielectric constant (ϵ_2). Hence the electronic transitions observed are assigned to indirect allowed transitions.
- The glass absorption cut-off wavelengths of MZLK glasses have shown blue shift whereas CZLK glasses have shown red shift with gradual change of $Li_2B_4O_7$ mole% in the glasses which are attributed to ion sizes and presence of various borate units present in the glass structure.
- The computed optical parameters E_{opt} , $\frac{N_c}{m^*}$, ϵ_1 , ω_p , E_d and E_0 have displayed non-linear linearities with a pronounced inflection at Li=K (30 mole% of alkali oxides) indicating mixed alkali effect (MAE) due to the presence of double alkali oxides in the glass network. The $\frac{N_c}{m^*}$ values indicated increasing free carrier concentrations revealing ion conducting nature of the present glass systems.

ACKNOWLEDGEMENTS

The authors thank the Head, Department of Physics, Osmania University, Hyderabad for providing experimental facilities and Principal, Vasavi College of Engineering (A), Hyderabad for providing sample preparation facilities.

References:

1. John C. Mauro, Edgar D. Zanotto, Two Centuries of Glass Research: Historical Trends, Current Status, and Grand Challenges for the Future, 5 (3) (2014)313–327 <https://doi.org/10.1111/ijag.12087>
2. Pillay R, Hansraj R, Rampersad N. Historical Development, Applications and Advances in Materials Used in Spectacle Lenses and Contact Lenses. Clin Optom (Auckl),12 (2020)157-167, <https://doi.org/10.2147/OPTO.S257081>
3. Kim D, Choi Y. Applications of Smart Glasses in Applied Sciences: A Systematic Review. Applied Sciences, 11(11) (2021)4956, <https://doi.org/10.3390/app11114956>.
4. Shyam Katnagallu, Ge Wu, Shiv Prakash Singh, Sree Harsha Nandam, Wenzhen Xia, Leigh T. Stephenson, Herbert Gleiter, Ruth Schwaiger, Horst Hahn, Michael Herbig, Dierk Raabe, Baptiste Gault, and Shanoob Balachandran, Nanoglass–Nanocrystal Composite—a Novel Material Class for Enhanced Strength–Plasticity Synergy, Small 16 (2020) 2004400, <https://doi.org/10.1002/sml.202004400>
5. Perepezko JH, Gao M and Wang J-Q, Nanoglass and Nanocrystallization Reactions in Metallic Glasses, Front. Mater, 8(2021)663862, <https://doi.org/10.3389/fmats.2021.663862>
6. Rammah, Y. S., F. I. El-Agawany, I. A. El-Mesady, Evaluation of photon attenuation and optical characterizations of bismuth lead borate glasses modified by TiO_2 Applied Physics A 125 (2019)727, <https://doi.org/10.1007/s00339-019-3023-9>
7. Shaik Kareem Ahmmad, M.A. Samee, Edukondalu. A, Syed Rahman, Physical and optical properties of zinc arsenic tellurite glasses, 2 (2012)175-181, <https://doi.org/10.1016/j.rinp.2012.10.002>
8. Saisudha B. Mallur, Tyler Czarniecki, Ashish Adhikari, Panakkattu K. Babu, Compositional dependence of optical band gap and refractive index in lead and bismuth borate glasses, Materials Research Bulletin 68 (2015) 27–34, <http://dx.doi.org/10.1016/j.materresbull.2015.03.033>
9. Murat Bengisu, Borate glasses for scientific and industrial applications: a review, J Mater Sci, 51(2016)2199–2242, <https://doi.org/10.1007/s10853-015-9537-4>
10. Donald, I.W., Mallinson, P.M., Metcalfe, B.L. et al. Recent developments in the preparation, characterization and applications of glass- and glass–ceramic-to-metal seals and coatings. J Mater Sci 46 (2011)1975–2000, <https://doi.org/10.1007/s10853-010-5095-y>
11. Jen-Hsien Hsu, Cheol-Woon Kim, Richard K. Brow, Joe Szabo, Ray Crouch, Rob Baird, An alkali-free barium borosilicate viscous sealing glass for solid oxide fuel cells, J. Power Sources, 270(2014)14-20.

12. Chambers, R.S., Gerstle, F.P., and Monroe, S.L. Viscoelastic Effects in a Phosphate Glass-. Metal Seal, *J. Amer. Ceram. Soc.*, 72[6] (1989) 929-32.
13. Mott N. F. and Davies E. A., *Electronic Processes in Non-Crystalline, Materials*, Clarendon Press, Oxford, (1979).
14. Sadeq, M.S., and Morshidy, H. Y., Effect of mixed rare-earth ions on the structural and optical properties of some borate glasses, *Ceramics International* 45 (2019) 18327–18332, <https://doi.org/10.1016/j.ceramint.2019.06.046>
15. Abouhaswa. A.S., Rammah, Y.S., Ibrahim, S.E., EL-Mallawany.R., Effect of mixed rare-earth ions on the structural and optical properties of some borate glasses, 45(15) (2019) 18327-18332, <https://doi.org/10.1016/j.ceramint.2019.06.046>
16. Padmaja, G., and Kistaiah, P, Infrared and Raman Spectroscopic Studies on Alkali Borate Glasses: Evidence of Mixed Alkali Effect. *The Journal of Physical Chemistry A*, 113(11) (2009), 2397–2404. <https://doi.org/10.1021/jp809318e>
17. Subhadra.M, Kistaiah.P, Infrared and Raman spectroscopic studies of alkali bismuth borate glasses: Evidence of mixed alkali effect, *Vibrational Spectroscopy*, 62(2012)23-27, <https://doi.org/10.1016/j.vibspec.2012.07.001>
18. Srinivas. B., Ashok Bhogi, Pallati Naresh, Abdul Hameed, M. Narasimha Chary, Md. Shareefuddin, Effect of SrO and TeO₂ on the physical and spectral properties of strontium tellurite boro-titanate glasses doped with Cu²⁺ ions, *Journal of Non-Crystalline Solids*, 575(2022)121218, <https://doi.org/10.1016/j.jnoncrysol.2021.121218>.
19. Yingtian Yu, John C. Mauro, Mathieu Bauchy, Stretched Exponential Relaxation of Glasses: Origin of the Mixed Alkali Effect, *American Ceramic Society Bulletin* 96, no. 4 (2017): 34-36, <https://doi.org/10.48550/arXiv.1801.01969>.